The 2014 World Congress on
Advances in Civil, Environmental, and Materials Research (ACEM14)
Busan, Korea, August 24-28, 2014

Flutter instability controls of long-span cable-supported bridge by investigating the optimum of fairing, spoiler and slot

Duy Hoa Pham[1)], *Van My Nguyen[2)]

[1)]*National University of Civil Engineering, Hanoi, Vietnam*
[2)]*Danang University of Science and Technology, Danang, Vietnam*
nvmy@dut.udn.vn

ABSTRACT

Aerodynamic instabilities are much important considerations in long span bridge design, where flutter instability has become the most important problem for cable bridges. One design approach is streamlining box girder cross-section with various aerodynamic attachments. In order to increase flutter stability, this paper proposes three technical solutions for the box girder cross-section of cable-supported bridge by varing the fairing angles, the ratios of spoiler width to bridge deck width and the ratios of slot width to bridge deck width. The problem was solved by applying computational fluid dynamics (CFD) method, known as “numerical wind tunnel”. Currently, methodology of CFD has gradually been accepted for analyzing the problem of interaction between wind flow and structures, especially for determining the aerodynamic parameters. This computational approach brought a good agreement with wind tunnel test results of Thuan Phuoc bridge, which is the longest suspension bridge of Vietnam, located in Danang city. By simulating many cross sections series with different fairing angles, spoilers, slots and bridge widths, it was found that flutter instability was prevented in some range of aerodynamic attachments dimensions.

1. INTRODUCTION

One of the methods used to solve the problem of interaction between structure and flow is Computational Fluid Dynamics (CFD, known as "numerical wind tunnel test". The fundamental of CFD is the basic laws of fluid dynamics. These basic principles can be expressed as mathematical equations under the form of partial derivative equation. Calculating fluid dynamics is a algorithms that replace partial equations of numerical fluid flow and put them in space and/or time to obtain a numerical description of flow field. Compared to the other methods, CFD is very useful in exhibiting clearly flow field and wind pressure distribution on the surface of the structures [2][5]. Moreover, CFD can also bring huge volume of calculations without spending much expenditure and so this is an ideal method for studying wind parameters. However, the accuracy of the CFD results should be verified by wind tunnel experiments.

[1)] Associate Professor
[2)] PhD scholar

For cable-supported bridges, flutter instability needs to be the great concern. Long-span bridges with non-streamlined cross-section and relatively large width and height ratio are sensitive with torsion flutter and coupled flutter. The difference in pressure between upper and lower sides of cross-section surface is considered the main mechanism causing flutter instability [1][3][4][6].

To counter with flutter instability, two different design solutions were proposed: (1) Fabricating the streamlined cross-sections (usually applied in Western European countries) to improve wind flow and bridge deck interactions and reduce the surface pressure difference of cross-section; (2) Using truss stiffening girder (usually applied in the United States and Japan) with the aims of increasing stiffness of the structures-wind flow as well as improve bending vibration frequency versus torsional frequency of structure. Besides that, it is necessary to investigate the optimal geometric parameters of the structure as well as the aerodynamic attachments to improve flutter stability. The paper investigated box sections to propose optimum about: (1) the fairing angle α (Fig. 1a); (2) the ratio of spoiler lengths and bridge deck widths (Fig. 1b); and (3) the ratios of slot width and bridge deck widths (Fig. 1c). These optimal parameters are much useful in the stage of preliminary design.

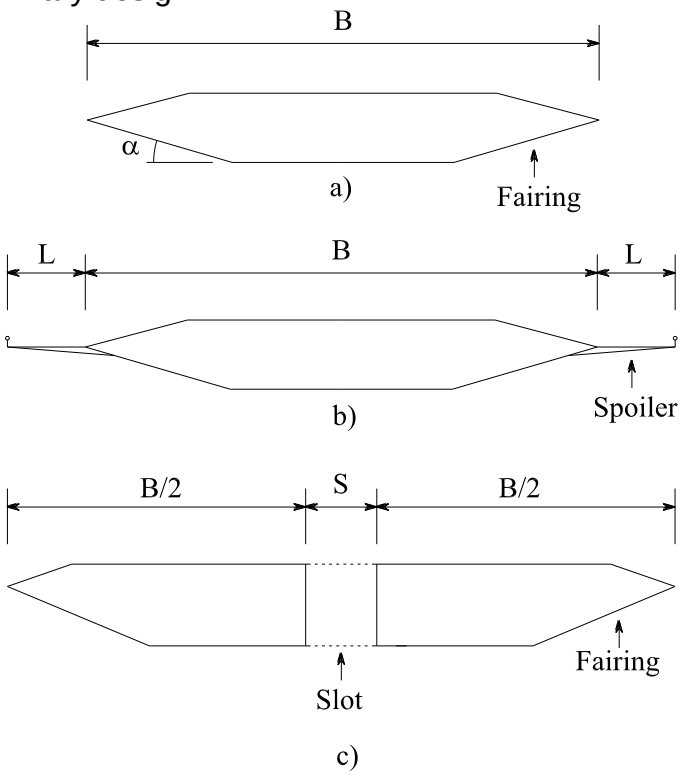

Fig. 1 Aerodynamic countermeasures: a) Fairing, b) Spoiler and c) Slot

2. MOTION EQUATION OF FLUTTER

2.1 Torsional flutter

The equation of motion of bridge deck for torsional flutter can be written as:

$$\ddot{\alpha}+2\xi_{0\alpha}\omega_{0\alpha}\dot{\alpha}+\omega_{0\alpha}^{2}\alpha=\frac{1}{2I}\rho U^{2}B^{2}\left(KA_{2}^{*}\frac{B\dot{\alpha}}{U}+K^{2}A_{3}^{*}\alpha\right), \tag{1}$$

where $\xi_{0\alpha}$ is the structural damping ratio, $\omega_{0\alpha}$ is the structural circular natural frequency in torsional vibration and I represents the mass moment of inertia of structure. From Eq. (1), the total damping ξ_{α} for the wind-structure system can be determined by:

$$\xi_{\alpha}=2\xi_{0\alpha}\omega_{0\alpha}-\frac{1}{2I}\rho UB^{3}KA_{2}^{*}, \tag{2}$$

and the Eq. (2) shows clearly that if bridge deck have positive A_{2}^{*}, the total damping may be negative. This causes vibration amplitude to increase until the bridge collapses. The critical torsional flutter wind speed can be calculated from Eq. (2).

2.2 Couple flutter

For a long-span cable-supported, flutter may involve multiple modes of vibration but the first vertical mode of vibration and the first torsional mode of vibration are often considered to be the most important [5]. The motion equation of bridge deck for coupled flutter can be written as:

$$\begin{aligned}\ddot{h}+2\xi_{0h}\omega_{0h}\dot{h}+\omega_{0h}^{2}h&=\frac{1}{2m}\rho U^{2}B\left(KH_{1}^{*}\frac{\dot{h}}{U}+KH_{2}^{*}\frac{B\dot{\alpha}}{U}+K^{2}H_{3}^{*}\alpha+K^{2}H_{4}^{*}\frac{h}{B}\right),\\ \ddot{\alpha}+2\xi_{0\alpha}\omega_{0\alpha}\dot{\alpha}+\omega_{0\alpha}^{2}\alpha&=\frac{1}{2I}\rho U^{2}B^{2}\left(KA_{1}^{*}\frac{\dot{h}}{U}+KA_{2}^{*}\frac{B\dot{\alpha}}{U}+K^{2}A_{3}^{*}\alpha+K^{2}A_{4}^{*}\frac{h}{B}\right),\end{aligned} \tag{3}$$

where ξ_{0h} is the structural damping ratio, ω_{0h} is the structural circular natural frequency in vertical vibration and m represents the mass of structure. By letting

$$C^{e}=\begin{bmatrix}2\xi_{0h}\omega_{0h}-\dfrac{\rho B^{2}L}{M}\omega_{h}H_{1}^{*} & \dfrac{\rho B^{3}L}{M}\omega_{\alpha}H_{2}^{*}\\ \dfrac{\rho B^{3}L}{I}\omega_{h}A_{1}^{*} & 2\xi_{0\alpha}\omega_{0\alpha}-\dfrac{\rho B^{4}L}{I}\omega_{\alpha}A_{2}^{*}\end{bmatrix}, \tag{4}$$

$$K^{e}=\begin{bmatrix}\omega_{0h}^{2}-\dfrac{\rho B^{2}L}{M}\omega_{h}^{2}H_{4}^{*} & \dfrac{\rho B^{3}L}{M}\omega_{\alpha}^{2}H_{3}^{*}\\ \dfrac{\rho B^{3}L}{I}\omega_{h}^{2}A_{4}^{*} & \omega_{0\alpha}^{2}-\dfrac{\rho B^{4}L}{I}\omega_{\alpha}^{2}A_{3}^{*}\end{bmatrix}. \tag{5}$$

The state matrix A can be expressed by

$$A = \begin{bmatrix} 0 & I \\ -K^e & -C^e \end{bmatrix}, \tag{6}$$

where I is the unit matrix. Through an iterative eignvalue analysis of A, the critical coupled flutter wind velocity can be determined.

3. BRIDGE DECK SIMULATION

3.1 Governing equations

The well-known Reynolds averaged Navier-Stokes (RANS) equations can be expressed for the incompressible fluid as follow:

$$\frac{\partial \bar{u}}{\partial x} + \frac{\partial \bar{v}}{\partial y} + \frac{\partial \bar{w}}{\partial z} = 0,$$

$$\rho\frac{\partial \bar{u}}{\partial t} + \rho\bar{u}\frac{\partial \bar{u}}{\partial x} + \rho\bar{v}\frac{\partial \bar{u}}{\partial y} + \rho\bar{w}\frac{\partial \bar{u}}{\partial z} = -\frac{\partial \bar{p}}{\partial x} + \mu\left(\frac{\partial^2 \bar{u}}{\partial x^2} + \frac{\partial^2 \bar{u}}{\partial y^2} + \frac{\partial^2 \bar{u}}{\partial z^2}\right) - \rho\frac{\partial \overline{u'u'}}{\partial x} - \rho\frac{\partial \overline{u'v'}}{\partial y} - \rho\frac{\partial \overline{u'w'}}{\partial z},$$

$$\rho\frac{\partial \bar{v}}{\partial t} + \rho\bar{u}\frac{\partial \bar{v}}{\partial x} + \rho\bar{v}\frac{\partial \bar{v}}{\partial y} + \rho\bar{w}\frac{\partial \bar{v}}{\partial z} = -\frac{\partial \bar{p}}{\partial y} + \mu\left(\frac{\partial^2 \bar{v}}{\partial x^2} + \frac{\partial^2 \bar{v}}{\partial y^2} + \frac{\partial^2 \bar{v}}{\partial z^2}\right) - \rho\frac{\partial \overline{v'u'}}{\partial x} - \rho\frac{\partial \overline{v'v'}}{\partial y} - \rho\frac{\partial \overline{v'w'}}{\partial z},$$

$$\rho\frac{\partial \bar{w}}{\partial t} + \rho\bar{u}\frac{\partial \bar{w}}{\partial x} + \rho\bar{v}\frac{\partial \bar{w}}{\partial y} + \rho\bar{w}\frac{\partial \bar{w}}{\partial z} = -\frac{\partial \bar{p}}{\partial z} + \mu\left(\frac{\partial^2 \bar{w}}{\partial x^2} + \frac{\partial^2 \bar{w}}{\partial y^2} + \frac{\partial^2 \bar{w}}{\partial z^2}\right) - \rho\frac{\partial \overline{w'u'}}{\partial x} - \rho\frac{\partial \overline{w'v'}}{\partial y} - \rho\frac{\partial \overline{w'w'}}{\partial z}, \tag{7a,b,c,d}$$

where $-\rho\overline{u'u'}$, $-\rho\overline{v'v'}$, $-\rho\overline{w'w'}$, $-\rho\overline{u'v'}$, $-\rho\overline{u'w'}$, $-\rho\overline{v'v'}$ and $-\rho\overline{v'w'}$ called Reynolds stresses are unknowns. To solve for the mean flow, they should be related to the time-averaged variables through turbulence models such as Spalart-Allmara, Standard k-ε, RNG k-ε, Wilcox k-ω, …

3.2 Simulation of Thuan Phuoc bridge deck

Thuan Phuoc bridge, which is the longest suspension bridge of Vietnam, has 405m-main span. The its cross-section is simulated with the rate of 1:50 compare to real dimensions. Table 1 shows parameters of this model. Reynolds number Re =1.59x10^6. The RNG k-ε model is applied in this computation.

Table 1 Parameters of section model

Parameter	Width	Height	Mass	Inertia mass	Radius of inertia	Basic vertical frequency	Basic torsional frequency
Unit	m	m	kg/m	kgm^2/m	m	Hz	Hz
Model	0.432	0.05	4.48	0.09237	0.144	2.11	5.76

Fig. 2 and Fig. 3 show the computational domain determined and mesh around bridge deck respectively. From the simulation results and calculations of the aerodynamic derivatives, Fig. 4 and Fig. 5 show the correlations between aerodynamic derivative and reduced wind speed, including the calculation results from wind tunnel tests for Thuan Phuoc bridge which implemented by Tongji University, China [8].

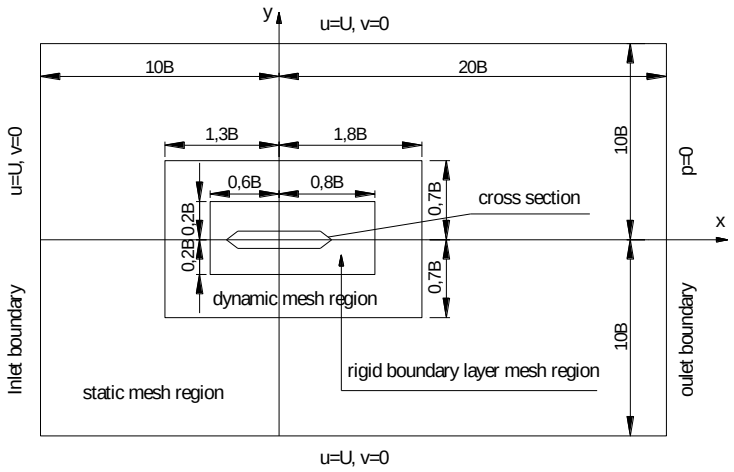

Fig. 2 Computational domain of bridge deck

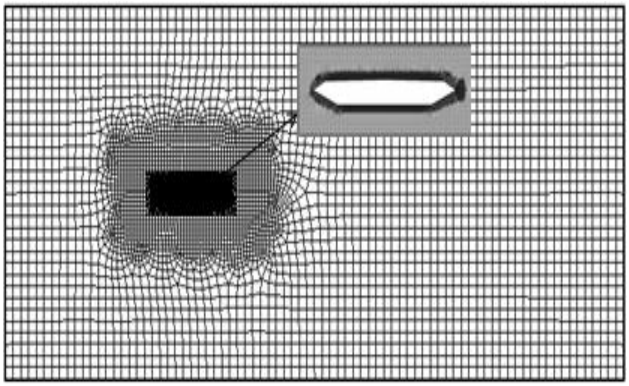

Fig. 3 Meshing around bridge deck

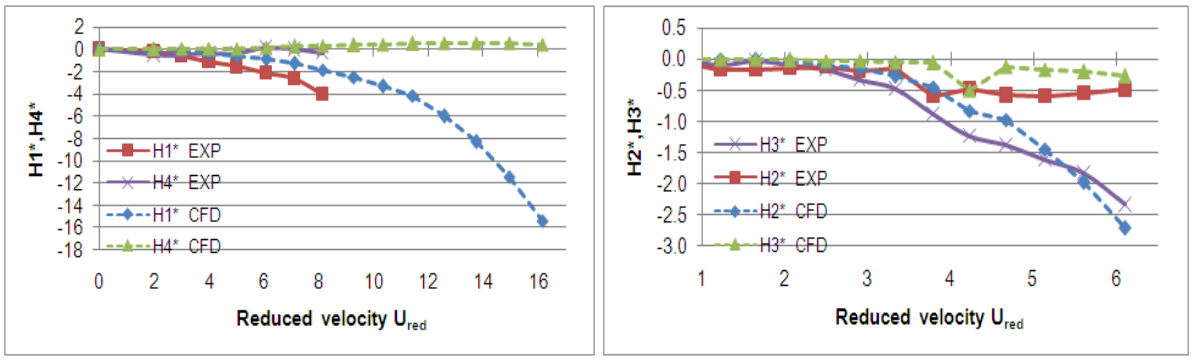

Fig. 4 Correlation of H_i^* (i=1-4) with reduced wind speed

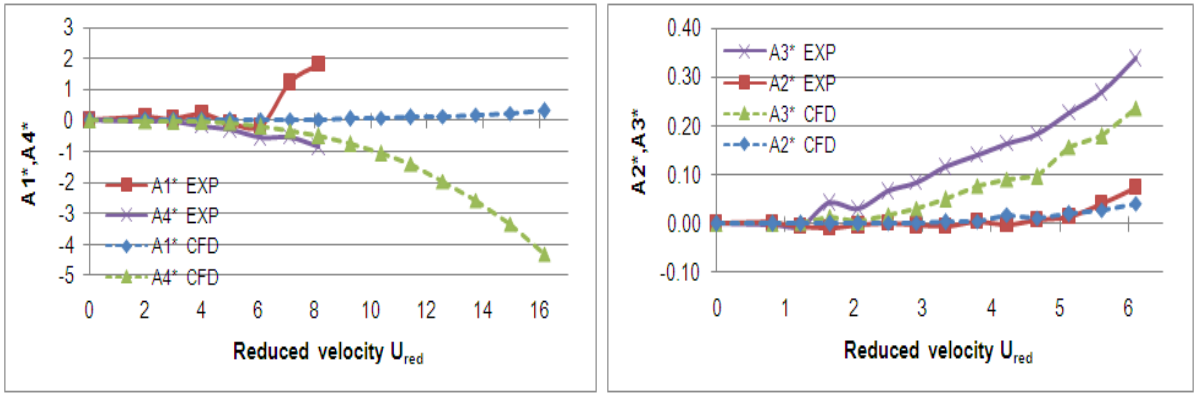

Fig. 5 Correlation of Ai* (i=1-4) with reduced wind speed

Furthermore, the results of flow-structure damping, shown in Fig. 6 to Fig. 8, are determined; and Table 2 displays the calculations of the critical flutter velocities for pure torsional (1DOF) motion and coupled (2DOF) motion.

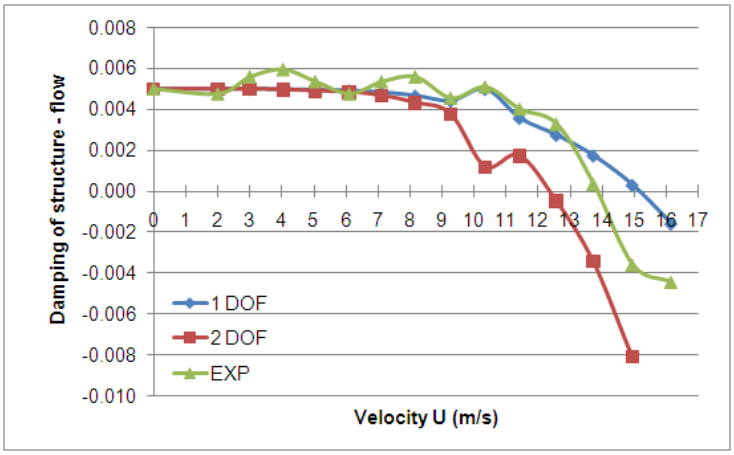

Fig. 6 Correlation of flow-structure damping with wind speed (attack angle $\alpha=0^{o}$)

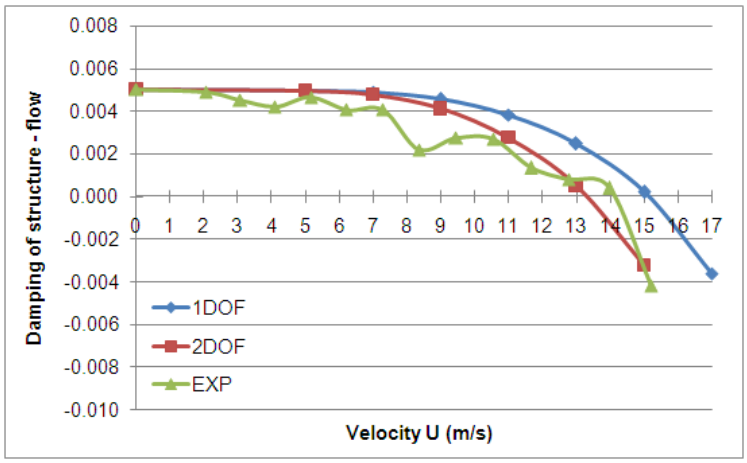

Fig. 7 Correlation of flow-structure damping with wind speed (attack angle $\alpha=-3^{o}$)

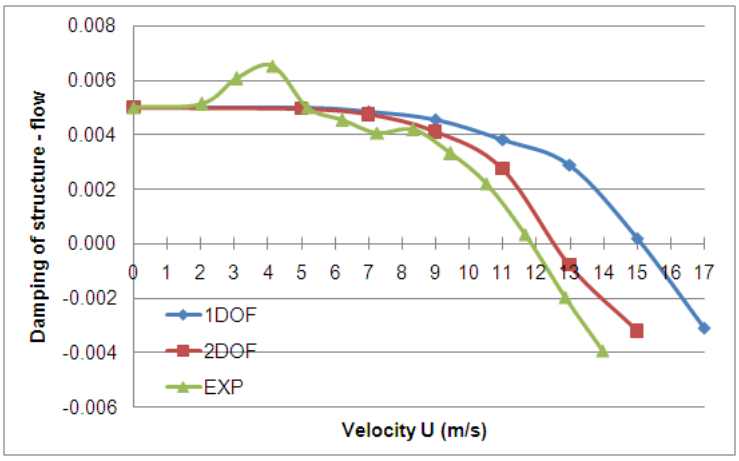

Fig. 8 Correlation of flow-structure damping with wind speed (attack angle α=+3^o)

Table 2 The critical flutter wind speed of Thuan Phuoc bridge deck

Attack angle α	The critical flutter wind speed (m/s)		
	Torsional flutter (1DOF) from simulation	Coupled flutter (2DOF) from simulation	Result from wind tunnel test [8]
-3^o	15.0	12.5	13.8
0^o	15.5	12.8	12.0
+3^o	15.2	13.4	14.1

As shown above, the CFD simulation results of Thuan Phuoc bridge deck are reliable compared to wind tunnel test.

4. INVESTIGATING THE OPTIMUM FAIRING, SPOILER AND SLOT

4.1 Investigate the optimized fairing angles (α)

The surveys was carried out with the different deck widths (B= 14.6m, 18.1m, 21.6m, 25.1m and 28.6m) and have to achieve the highest critical fultter wind speeds. In accordance with fairing angle (α) changes from 18^o to 27^o (Fig.1a), Fig. 9 illustrates the relationship between the ratio $U_{cri,i}/U_{cri,18}$ with different widths, where $U_{cri,i}$ is the critical wind speed at the ith angle and $U_{cri,18}$ is the critical wind speed at fairing angles α = 18^o.

From Fig. 9, it can be seen that the larger deck widths, the more flutter instability structures exhibit. Furthermore, fairing shape is not so sensitive to flutter stability and critical wind speed increased by 2% - 6%. The optimal fairing angle domain is from 21^o – 24^o and as fairing angle is larger than about 25^o the critical wind velocity will decline.

4.2 Investigate the optimized ratio of spoiler length and bridge deck width

Together with the various bridge widths as section 4.1, the length of spoiler L is surveyed with ratio L/B = 0, 0.05, 0.06, 0.07, 0.08, 0.09 and 0.10 respectively (Fig. 1b). Fig. 10 shows the relationship between the rate $U_{cri,i}/U_{cri,0}$ over different widths (B),

where $U_{cri,i}$ is the critical wind speed with L/B and $U_{cri,0}$ the critical wind speed with L/B=0.

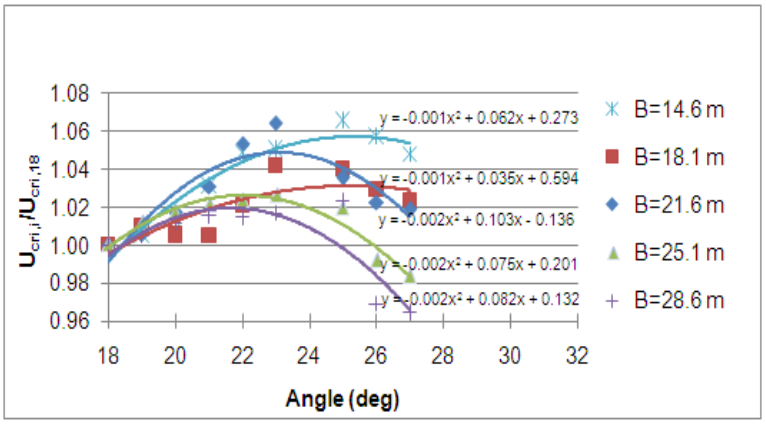

Fig. 9 The regression line $U_{cri,i}/U_{cri,0}$ is the function of fairing angles (α) with different widths (B)

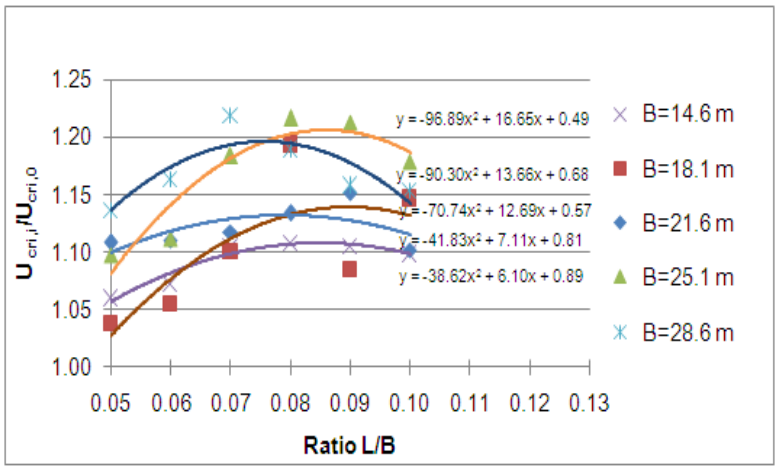

Fig. 10 The regression line $U_{cri,i}/U_{cri,0}$ is the function of L/B with various widths

From Fig. 10, it is clear that the wider bridge deck width, the more flutter instability structures obtain. Besides that, using the spoiler can improve flutter stability effectively rather than changing fairing angle. Moreover, the optimization ratio L/B is from 0.07 to 0.09 and the critical wind speed increased by 10% - 20% compared to the fairing. As the ratio (L/B) is greater than 0.09, critical wind speed will be decreased.

4.3 Investigate the optimized ratio of slot width and bridge deck width

The surveys was carried out with the different deck widths (B= 18.1m, 21.6m, 25.1m, 28.6m and 35.1m). In accordance with ratio S/B changes 0, 0.01, 0.015, 0.02, 0.03 and 0.04 (Fig.1c), Fig. 11 illustrates the relationship between flow-structure damping with different widths and Fig. 12 shows the relationship between the rate $U_{cri,i}/U_{cri,0}$ over

different ratios S/B, where $U_{cri,i}$ is the critical wind speed with L/B and $U_{cri,0}$ the critical wind speed with S/B=0.

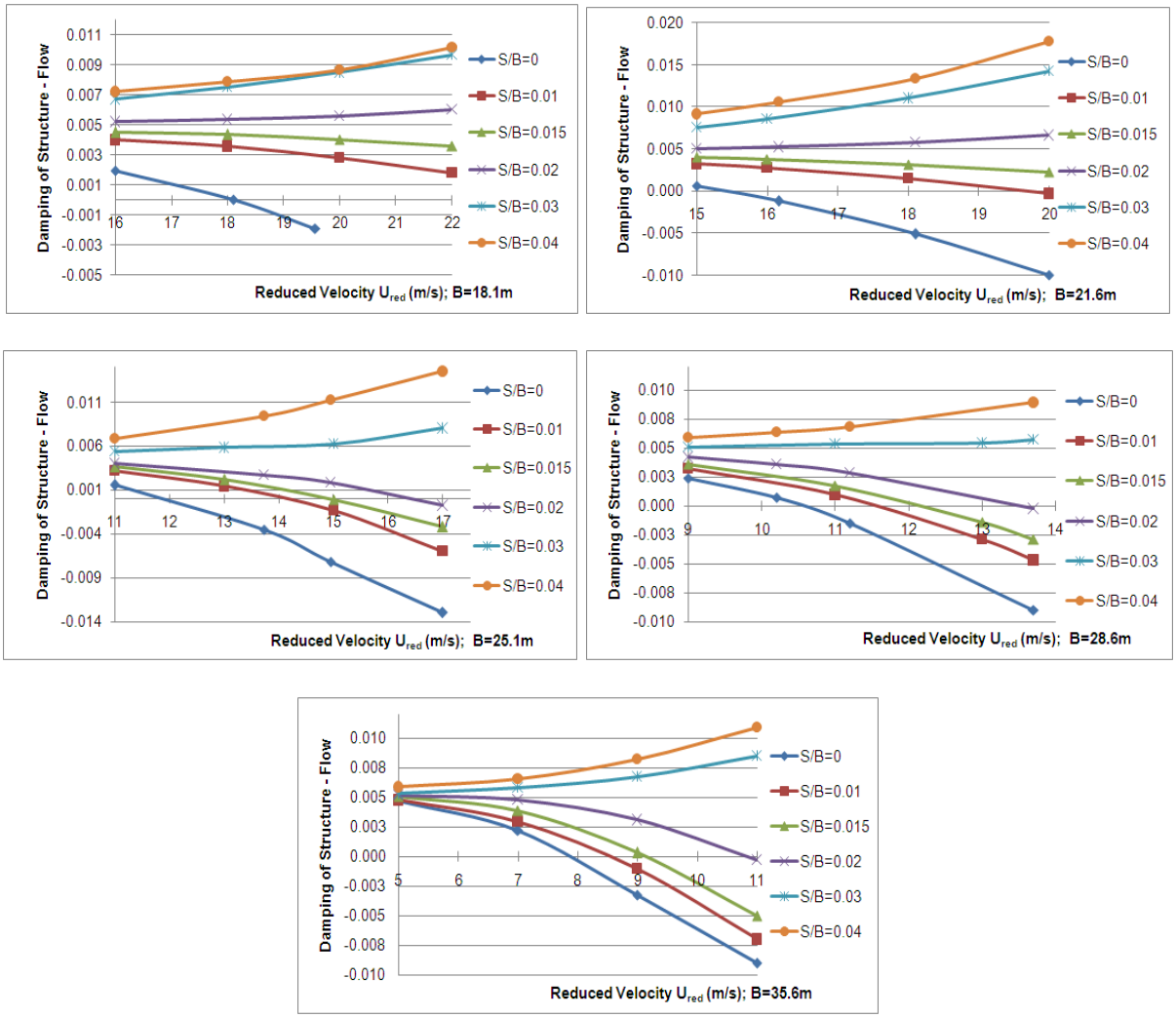

Fig. 11 Correlation of flow-structure damping with ratio S/B in accordance with various widths

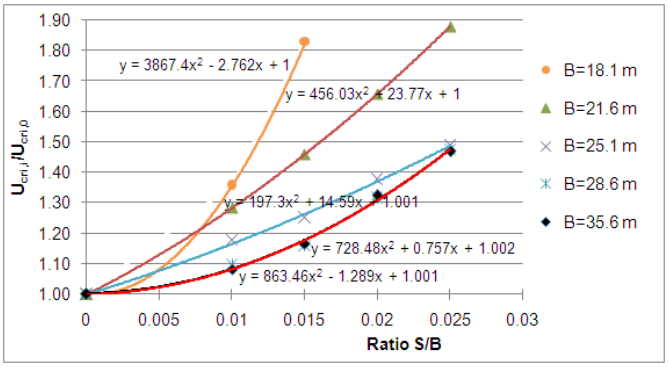

Fig. 12 The regression line $U_{cri,i}/U_{cri,0}$ is the function of S/B with various widths

From Fig. 10 and Fig. 12, it is also clear that the wider bridge deck width, the more flutter instability structures obtain. Besides that, using the center slot can improve flutter stability effectively rather than changing angle α and ratio L/B. Moreover, the optimization ratio S/B is not less than S/B=0.03.

5. CONCLUSIONS

Methodology of computational fluid dynamics (CFD) has gradually been accepted to analyze the problem of interaction between wind flow and structures, especially for determining the aerodynamic parameters.
The paper proposes optimum about the fairing angle ($\alpha = 21^o–24^o$), the ratio of spoiler lengths and bridge deck widths (L/B = 0.07-0.09) and the ratios of slot width and bridge deck widths (S/B $\geq$0.03). These optimal parameters are much useful in the stage of preliminary design.

REFERENCES

[1] Yozo Fujino, Dionysius Siringringo (2013), “Vibration Mechanisms and Controls of Long-Span Bridges: A Review”, *Structural Engineering International 3/2013*.
[2] Jens Honoré Walther, Allan Larsen (1997), “Two dimensional discrete vortex method for application to bluff body aerodynamics”, *Journal of Wind Engineering and Industrial Aerodynamics* 67&68 (1997) 183-193.
[3] Giuseppe Vairo (2003), “A Numerial Model for Wind Loads Simulation on Long-Span Bridges”, *Elsevier, Simulation Modelling Practice and Theory 11 (2003)* 315-351.
[4] J.A. Juarado, S. Hermández, F. Nieto & A. Mosquera (2011), “Bridge Aeroelastiity: Sensitivity Analysis and Optimal Design”, *WIT Press, Great Britain*.
[5] Claudio Mannini (2008), “Flutter Vulnerability Assessment of Flexible Bridges”, *VDM Verlag Dr. Muller Aktiengesellschaft & Co. KG*.
[6] You-Lin Xu (2013), “Wind Effects on Cable-Supported Bridges”, *Wiley*.
[7] Fujino Y, Kimura K, Tanaka H (2012), “Wind Resistant Design of Bridges in Japan: Development and Practices”, *Springer*.
[8] Tongji University (2003), “Wind tunnel study on wind-resistant performance of the Thuan Phuoc bridge in Danang city, Vietnam”.